

BISPECTRAL TRANSFER FUNCTION OF THE PATH OF SIGNAL PROPAGATION THROUGH A CLOUD LAYER

O.I. Aldoshina, V.V. Bacherikov, A.N. Karkhov, and V.A. Fabrikov

*All-Union Scientific-Research Institute of Optophysical Measurements, Moscow
Received May 12, 1991*

Propagation of signals from a point isotropic source of incoherent unpolarized optical radiation through the atmosphere with a homogeneous cloud layer of large optical thickness is modeled. An analytic expression is obtained for the bispectral transfer function of such a path. The function is plotted at various observation angles.

1. Propagation of signals from a point isotropic source of incoherent unpolarized optical radiation through the atmosphere with a homogeneous cloud layer of large optical thickness ($\tau > 10$) to a detector removed at "infinity" is modeled. We will regard the propagation path as a linear system, invariant with respect to shifts in time, which may be characterized in temporal and frequency domains by its impulse response and transfer function, respectively. When the transfer function of the path $H(\omega)$ is well known, one may calculate its bispectral transfer function

$$H^3(\omega_1, \omega_2) = H(\omega_1) H(\omega_2) H(-\omega_1 - \omega_2) \quad (1)$$

which is a characteristic of such a system widely used to reconstruct signals and images.¹⁻⁴ Triplet correlation functions and bispectra in signal processing are effective means of suppressing the additive noise.¹ The noise is suppressed to such a degree that it becomes possible to extrapolate the spectrum of the signal outside the frequency band of the system by the method of analytic continuation, expanding the spectrum in a series in terms of the prolate spheroidal functions.^{5,6}

The aim of our study is to find an analytic expression for $H(\omega)$ and to construct the bispectral transfer function of the path on this basis. Our treatment is based on the model developed in Ref. 7.

2. We search for the spatiotemporal distribution of the intensity of radiation at the top of the cloud layer

$$I(x, y, t; \omega) = I(x, y; \omega) e^{i\omega t} \quad (2)$$

when the source generates a signal with the envelope $\exp(i\omega t)$. If we specify the distribution in the reference system affixed to the detector, the input signal of the detector, to within the constant k , independent of x and y , can be obtained by integrating Eq. (2) over x and y . Then

$$H(\omega) = \kappa \int_{-\infty}^{\infty} \int_{-\infty}^{\infty} I(x, y; \omega) dx dy, \quad (3)$$

where

$$\kappa = \Omega \cos \theta / \pi, \quad (4)$$

Ω is the aperture angle of the detector, θ is the angle between the direction of the detector and the normal to the surface of the layer. We assume scattering of radiation by the cloud layer to be Lambertian and the detector to be removed at the "infinitely" large distance L from the scatterer. The first assumption holds at optical depths $\tau > 10$, and the second one – for $L > h_0$, where h_0 is the height of the cloud layer top above the source (see Fig. 1).

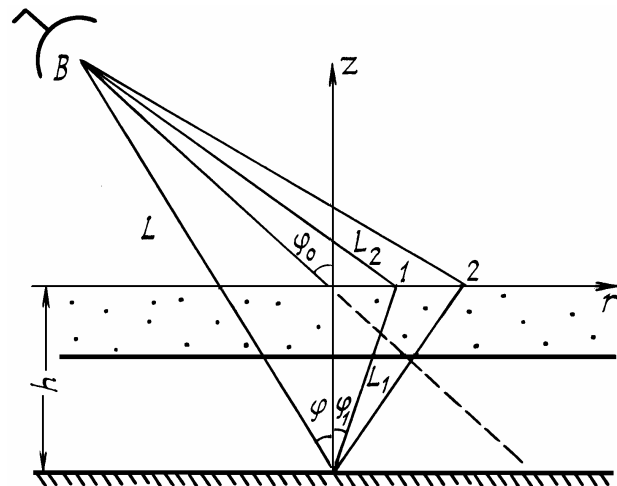


FIG. 1. The scheme of observing a nonstationary isotropic radiation source through a cloud layer.

In case of an isotropic point source and completely absorbing underlying surface the illumination at the cloud bottom $I_0(r')$ obeys the distribution

$$I_0(r') = C/R^3, \quad R = (1 + r'^2/h_0^2)^{1/2}, \quad (5)$$

$$r = (x^2 + y^2)^{1/2}, \quad r' = r \frac{h_0 - \Delta h}{h_0},$$

where Δh is the thickness of the cloud layer.

The constant C can be found from the condition of normalization

$$2\pi \int_{-\infty}^{\infty} r' I_0(r') dr' = 1/2, \quad r' dr' = h_0^2 R dR; \quad C = 1/4\pi h_0^2.$$

The source power is taken to be unity in this case.

The intensity distribution at the top of the cloud $I(r) = I(r, 0)$ may be obtained from Eq. (5) by the method of angular zones⁸ with the use of the well-known analytic solution of the problem of radiative transfer of unidirectional beams⁹ through a plane-parallel medium. Regarding the radiation from the source as a superposition of independent unidirectional beams intersecting the cloud layer bottom at the angle $\phi = \arccos \mu_0$, which depends on the coordinate r as

$$\mu_0 = 1/R = (1 + r^2/h_0^2)^{-1/2}, \quad (7)$$

and introducing the weighting functions

$$w(r) = C/R^2 = 1/4\pi h_0^2 (1 + r^2/h_0^2),$$

we obtain for the single-scattering albedo $\tilde{\omega}_0 = 1$

$$I(r) = \frac{\mu_0^3}{(2\pi h_0)^2} \left\{ \frac{1 - 4\mu_0^2}{4(\mu - \mu_0)} (e^{-\tau_1/\mu} - e^{-\tau_1/\mu_0}) + C_1(1 - \tau_1 - e^{-\tau_1/\mu}) + C_2(1 - e^{-\tau_1/\mu_0}) \right\}; \quad (8)$$

$$C_1 = \frac{1 + 2\mu_0 + (1 - 2\mu_0)e^{-\tau_1/\mu_0}}{2(1 + \tau_1)},$$

$$C_2 = \frac{(1 + 2\tau_1)(1 + 2\mu_0) - (1 - 2\mu_0)e^{-\tau_1/\mu_0}}{4(1 + \tau_1)}, \quad \mu = \cos\theta;$$

where τ_1 is the optical thickness of the layer, μ_0 corresponds to the cosine of the angle of the beams incident upon the cloud layer bottom at the points removed at the distance r from the central line OZ (Fig. 1), $w(r) = C\mu_0^2$ is the density of the radiant flux propagating from the source in the direction (μ_0, ϕ) . In the asymptotic approximation of large optical thicknesses $\tau_1 \rightarrow \infty$, Eqs. (8) are reduced to the form

$$I(r) = \frac{C}{2\pi} \eta \frac{1}{R^3} \left(1 + \frac{2}{R} \right), \quad \eta = \frac{3}{2(1 + \tau_1)}, \quad (9)$$

where R and C are determined by formulas (5) and (6). Formulas (8) and (9) describe, to a satisfactory accuracy, the spatial distribution of brightness of the cloud layer $I(r)$ (the error does not exceed 10%) rather than the dependence of I on μ . This dependence is manifested in the higher order approximation alone. Its account affects the factor k entering into Eq. (3) without changing the form of the function $H(\omega)$.

To make our calculations more convenient, we approximate formula (9) by the relation

$$I(r) = \frac{C_0}{R} \exp(-R/R_0), \quad (10)$$

where

$$C_0 = \frac{1}{(2\pi h_0)^2} \eta \frac{1}{R_0} e^{1/R_0}, \quad R_0 = 2/3. \quad (11)$$

The constants C and R_0 are chosen so as to keep unchanged the value $I(0)$ and the area under the curve $I(r, \phi)$.

To find $I(r, \omega)$ we must take into account the time delay $\Delta(r, \omega)$ caused by the geometric path difference between the rays passing through different points (r, ϕ) at the top of the cloud layer

$$\Delta(r, \phi) = \frac{L_1 + L_2 - L}{c} = t_0 (R + \sqrt{R^2 - 1} \sin\theta \cos\phi - \cos\theta), \quad (12)$$

$$t_0 = h_0/c$$

Here c is the velocity of light and L_1 , L_2 , and L are the distances $A1$, $1B$, and AB , respectively (see Fig. 1). The

impulse response of the medium to the unidirectional beams should also be taken into account. It is approximated by the relation

$$\psi(t; r, \phi) = \frac{t'}{T^2} e^{-t'/T} U(t'), \quad t' = t - \Delta(r, \phi), \quad (13)$$

where $U(t')$ is the Heaviside function, T is the constant given by formulas¹⁰

$$T = T(r) = \frac{t_1 \tau_1}{4\alpha_p} R^2, \quad (14)$$

$$t_1 = \Delta h / c, \quad \alpha_p \approx 2.66 (D/\lambda)^2,$$

and D is the effective diameter of cloud particles.

The error in approximating the calculated data, borrowed from Ref. 9, by the function $\psi(t; r, \phi)$ does not exceed 15%.

The Fourier transform of the function $\psi(t; r, \phi)$ is given by the formula

$$H_0(\omega; r, \phi) = \frac{1}{(i\omega T + 1)^2} e^{-i\omega\Delta(r, \phi)} \quad (15)$$

and

$$I(r, \phi; \omega) = I(r) H_0(\omega; r, \phi). \quad (16)$$

In the limiting case of small T , the impulse response of the medium to the unidirectional beams tends to ward the Dirac delta function $\delta[t - \Delta(r, \phi)]$, and the function $H_0(\omega; r, \phi)$ – to ward the exponential dependence $\exp[-i\omega\Delta(r, \phi)]$.

3. Based on Eqs. (10), (15), and (16) and the Bessel formula

$$\frac{1}{2\pi} \int_0^{2\pi} e^{-iv \cos\phi} d\phi = J_0(v)$$

Eq. (3) is reduced to the form

$$H(\omega) = A e^{i\omega t_0 \cos\theta} \int_1^\infty e^{-pR} J_0(\omega t_0 \sin\theta \sqrt{R^2 - 1}) \frac{1}{(i\omega T + 1)^2} dR, \quad (17)$$

$$A = \Omega \frac{\cos\theta}{2\pi} \eta \frac{1}{R_0} e^{1/R_0}, \quad p = 1/R_0 + i\omega t_0.$$

Substituting the characteristic value

$$\tilde{T} = \frac{t_1 \tau_1}{4\alpha_p \cos^2\theta}, \quad (18)$$

corresponding to the shortest ray path length, into Eq. (17) for the variable T , and taking the constant outside the integral, we obtain:

$$H(\omega) = A e^{i\omega t_0 \cos\theta} \frac{1}{(i\omega \tilde{T} + 1)^2} \frac{\exp(-\sqrt{p^2 + (\omega t_0 \sin\theta)^2})}{\sqrt{p^2 + (\omega t_0 \sin\theta)^2}}. \quad (19)$$

The impulse response of the system with the transfer function given by Eq. (17) can be represented by the convolution of two functions

$$f(t) = F^{-1}[H(\omega)] = f_1(t) * f_2(t), \quad (20)$$

$$f_1(t) = \frac{A}{t_0 \cos \theta} e^{-b\beta} I_0(b \sin \theta \sqrt{\beta^2 - 1}) U(t),$$

$$f_2(t) = \frac{t}{T^2} e^{-t/T} U(t),$$

$$\beta = t/t_0 \cos \theta + 1, \quad b = 1/R_0 \cos \theta; \tag{21}$$

and I_0 is the modified zero the order Bessel function of the first kind.

If $A(\omega)$ is the modulus and $\psi(\omega)$ is the argument of the transfer function (19), i.e.,

$$H(\omega) = A(\omega) e^{i\psi(\omega)}, \tag{22}$$

than

$$A(\omega) = \eta \frac{\kappa}{2} \frac{\exp[(1 - a \cos \Psi)/R_0]}{a} \frac{1}{(\omega^2 T^2 + 1)},$$

$$\Psi(\omega) = \Psi + \Psi_0 + \frac{a \sin \Psi}{R_0} - \omega t_0 \cos \theta, \tag{23}$$

where

$$\Psi = \begin{cases} a = [(1 - R_0^2 x_0^2 \cos^2 \theta)^2 + (2R_0 x_0)^2]^{1/4}, \\ \frac{1}{2} \arctan \frac{2R_0 x_0}{1 - (R_0 x_0 \cos \theta)^2}, R_0 x_0 \cos \theta \leq 1, \\ \frac{1}{2} \arctan \frac{2R_0 x_0}{1 - (R_0 x_0 \cos \theta)^2} + \frac{\pi}{2}, R_0 x_0 \cos \theta > 1, \\ \Psi_0 = 2 \arctan \omega \tilde{T}, x_0 = \omega x_0. \end{cases} \tag{24}$$

4. So far we neglected the reflecting properties of the underlying surface. The effect of the Lambertian surface with albedo $B \neq 0$ may be accounted for following the technique described in Ref. 7. We then obtain the computational relations

$$H(\omega) = \eta \frac{\kappa}{2} \frac{P_0(\omega) + B P_1(\omega)}{1 - B(1 - \eta) P_2(\omega)},$$

$$P_0(\omega) = H_0(x_0) e^{i\nu_0 \cos \theta}, \quad P_2(\omega) = H_3^2(x_1),$$

$$P_1(\omega) = H_1(x_1 - x_0) H_2(x_1) e^{i\nu_0 \cos \theta}, \tag{25}$$

where

$$H_k(x_i) = \frac{1}{(\omega \tilde{T})^2 + 1} \frac{\exp \left[\frac{1}{R_k} (1 - \sqrt{1 - (R_k x_i \cos \theta)^2} + i 2 x_i R_k) \right]}{\sqrt{1 - (R_k x_i \cos \theta)^2} + i 2 x_i R_k},$$

$$x_0 = \omega h_0 / c, x_1 = \omega h_1 / c,$$

$$R_0 = 2/3, R_1 = 1, R_3 = 1/2. \tag{26}$$

Here the function $H(\omega)$ is represented in terms of its modulus and argument in exactly the same way as for $B = 0$.

5. Figures 2 and 3 graphically present the results of calculations of the bispectral transfer function of the path normalized by the value $(k\eta/2)^3$ at two zenith angles of 0° and 60° for the following values of the parameters of clouds and underlying surface: $h_0 = 0.7$ km, $\eta = 0.2$, $h_1 = 1$ km, $B = 0.35$, and $\Delta h = 1$ km. With the symmetry of bispectra associated with their evenness in the arguments ω_1 , ω_2 , and $\omega_1 + \omega_2$, taken into account these graphs are presented for one quadrant alone.

As can be seen from these figures, when the zenith angle θ increases from 0 to 60° , the spectra get narrower and closer to the zero point in the frequency plane. This result follows logically from longer impulse responses at larger θ .

6. Analytic relations (1) and (22)–(26) completely determine the bispectral transfer function of the propagation path of the signals of the above-considered type. They can be employed in computer programs designed for recording the signals propagated through the atmospheric cloud layers and for retrieving their actual shape. They are applicable to pulses of optical radiation generated by sources with wide directivity pattern.

Formulas (22)–(26) are model. To obtain them, numerous simplifications and assumptions were introduced, and within the developed formalism not all of them may be estimated comprehensively enough. The proposed analytic solutions must be compared with more cumbersome but more accurate numerical results based on the direct solutions of the corresponding radiative transfer equations.

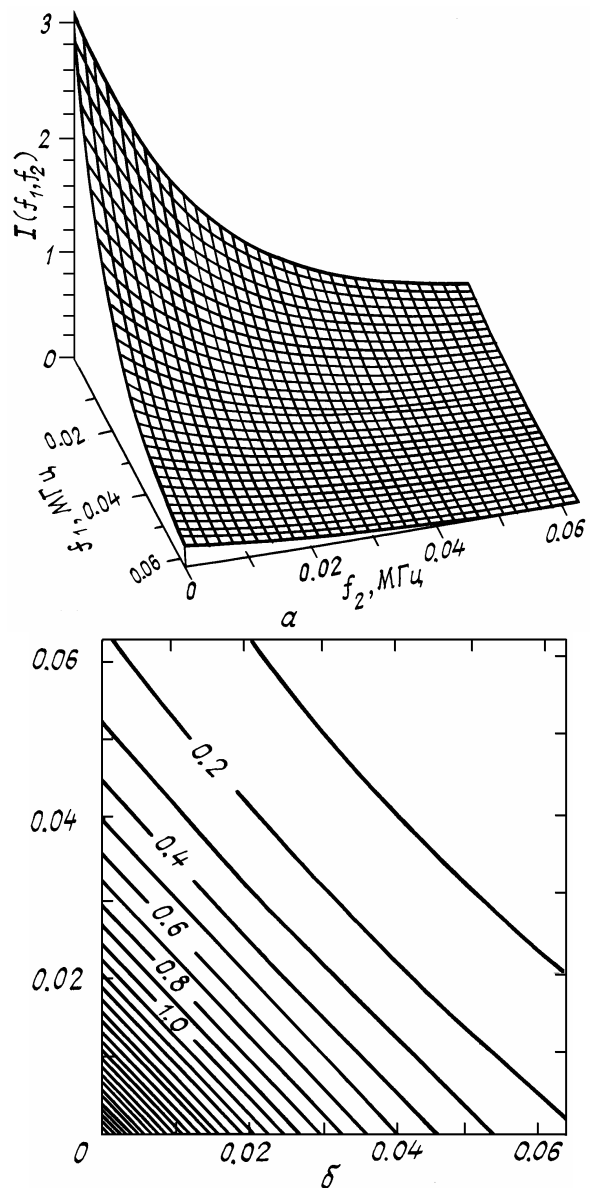


FIG. 2. Bispectrum of the path at $\theta = 0^\circ$.

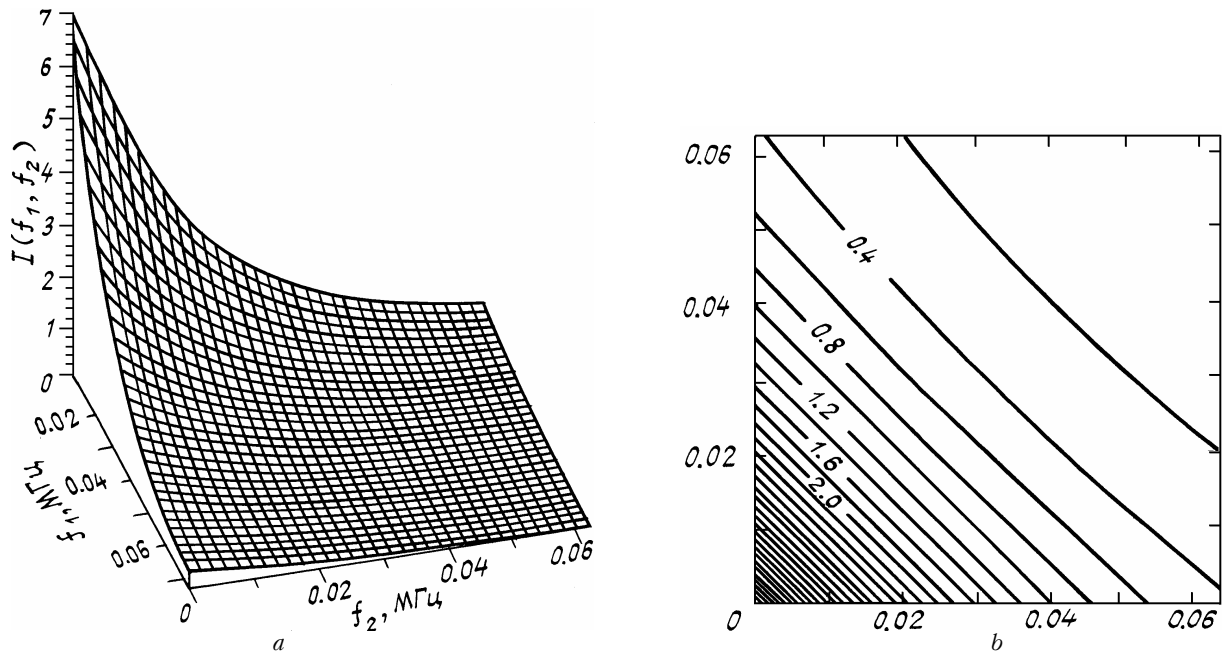


FIG. 3. Bispectrum of the path at $\theta = 60^\circ$.

REFERENCES

1. A.V. Lomann and B. Wirnittser, *Proc. IEEE* **72**, No. 7, 158–173 (1984).
2. M.J. Hinich, *IEEE Transactions on Acoustics, Speech, and Signal Processing* **38**, No. 7, 1277–1283 (1990).
3. R. Barakat and S. Ebstein, *J. Opt. Soc. Am.* **A4**, No. 9, 11756–1763 (1987).
4. S. Alshebeili and A.E. Cetin, *IEEE Transactions on Geoscience and Remote Sensing* **28**, No. 2, 166–170 (1990).
5. A. Tockij, J. Perina, and S. Zabura, *Optik* **83**, No. 3, 85–87 (1989).
6. B.R. Frieden, in: *Progress in Optics*, E. Wolf, ed., (North Holland, Amsterdam, Publ. Co., 1971), Vol. 9, pp. 313–411.
7. O.I. Aldoshina, V.V. Bacherikov, A.N. Karkhov, et al., *Atm. Opt.* **3**, No. 5, 490–497 (1990).
8. K.S. Adzerikho, *Inzh.–Fiz.Zh.* **57**, No. 2, 653–658 (1989).
9. J.S. Chou, *Appl. Opt.* **17**, No. 3, 364–373 (1978).
10. A. Ishimari, *Wave Propagation and Scattering in Randomly Inhomogeneous Media* [Russian translation] (Mir, Moscow, 1981), Vol. 2, 317 pp.